



#### ■ Author(s)

Yuceturk GD<sup>1</sup>  <https://orcid.org/0000-0002-7717-7977>

<sup>1</sup> Department of Environmental Engineering, Faculty of Engineering, Bolu Abant İzzet Baysal University, 14030, Bolu, Türkiye.

#### ■ Mail Address

Corresponding author e-mail address  
Gamze Dogdu Yuceturk  
Department of Environmental Engineering,  
Faculty of Engineering, Bolu Abant İzzet  
Baysal University, 14030, Bolu, Türkiye.  
Phone: +903742534558  
Email: [gamzedogdu@ibu.edu.tr](mailto:gamzedogdu@ibu.edu.tr)

#### ■ Keywords

Ammonia removal, Cost analysis, Hydrogen peroxide-sono-photocatalysis, Phosphorus elimination, Poultry slaughterhouse wastewater.



Submitted: 27/December/2023  
Approved: 26/February/2024

# Integrated Hydrogen Peroxide, Sono, and Heterogeneous Photocatalysis Technologies: A Novel Technique for Ammonia and Phosphorus Removal in Real Poultry Slaughterhouse Wastewater

## ABSTRACT

Poultry slaughterhouse wastewater (PSW) has substantial organic load and nutrient contents, which must be removed before discharge due to being sanitary and environmental hazards. The present study is the first to analyze the individual and synergistic influences of combined hydrogen peroxide (H<sub>2</sub>O<sub>2</sub>), different ultraviolet lights (UV-A/UV-C), inorganic compound catalysts of titanium and zinc oxides (TiO<sub>2</sub>/ZnO), and ultrasound (US) processes on ammonia and phosphorus elimination from PSW using a Taguchi L<sub>36</sub> orthogonal array. The results showed that, compared to other processes in isolation, the integrated process of H<sub>2</sub>O<sub>2</sub>, US, and heterogeneous photocatalysis (HPC) is significantly more effective at treating PSW in terms of N<sub>4</sub><sup>+</sup>-N removal (52.0%) and PO<sub>4</sub>-P elimination (59.5%). Furthermore, electrical energy consumption at 2.67 g<sup>-1</sup> N<sub>4</sub><sup>+</sup>-N US\$ and 2.14 g<sup>-1</sup> PO<sub>4</sub>-P US\$ was determined to be the most significant factor in the operating cost of the system, while the average chemical cost under optimal conditions was 0.34 US\$/g. In general, the results indicate that the effectiveness of removing pollutants is directly influenced by the pH, catalyst concentration, and duration of the operation. Additionally, the presence of different types of pollutants in real wastewater might lead to reduced nutrient removal efficiencies.

## INTRODUCTION

Poultry meat is one of the primary animal protein sources for many people in most countries due to its nutritional and sensory properties, affordability, ease of preparation, and absence of religious restraints (OECD, 2023). FAO (2023) declared that the poultry meat production sector increased from 133.6 million tons in 2019 to 136.0 million tons in 2020. However, the processing of poultry includes slaughtering, de-feathering, evisceration, washing, and chilling steps that generate large amounts of wastewater that is characterized by high loads of organic components, with chemical oxygen demand (COD) measured between 1,250 and 15,900 mg/L (Bustillo-Lecompte *et al.*, 2016; Abdelhay *et al.*, 2020); biological oxygen demand (BOD) concentration of 1,602 mg/L (Yaakob *et al.*, 2018); ammonium-N (N<sub>4</sub><sup>+</sup>-N) concentration of 53–312 mg/L (Ngobeni *et al.*, 2022); and orthophosphate (PO<sub>4</sub>-P) concentration of 9.65 mg/L (Bayar *et al.*, 2022). Additionally, based on previous research (Rinquest *et al.*, 2019; Williams *et al.*, 2019), it is expected that 80-90% of a processing plant's total water use will be discharged as poultry slaughterhouse wastewater (PSW), consuming an average of 26.5 L per processed bird (Fatima *et al.*, 2021). Ionized ammonia (N<sub>4</sub><sup>+</sup>) and free ammonia (NH<sub>3</sub>) are the two forms of reduced inorganic nitrogen found in the aqueous medium, which can exist in water as ammonia gas or as water soluble ammonia ions (Purwono *et al.*, 2023). The majority of phosphorus in natural water and wastewater



exists in the form of orthophosphate ions ( $\text{PO}_4^{3-}$ ), specifically  $\text{H}_2\text{PO}_4^-$ ,  $\text{HPO}_4^{2-}$ , and  $\text{PO}_4^{3-}$  that originates from poultry manure, meat, and bone meal (Topcu *et al.*, 2022). The removal of nutrients such as ammonia and phosphate from PSW has emerged as a prominent area of investigation, as evidenced by the attention it has received in recent studies (Hajaya and Pavlostathis, 2013; Türkdoğan *et al.*, 2018). Despite the many different available techniques, such as dissolved air flotation (DAF), electrocoagulation (EC), coagulation-flocculation (CF), aerobic and anaerobic processes, membrane techniques, reverse osmosis, etc., the toxicity of this type wastewater continues to be inadequate, with contaminant levels after treatment above the legally permitted values (Meiramkulova *et al.*, 2020; Musa *et al.*, 2021; TeránHilares *et al.*, 2021; Ngobeni *et al.*, 2022; Toh *et al.*, 2023). In addition, high operational and maintenance costs, low efficiency in solid-liquid separation, high chemical requirements, high sludge generation, long hydraulic retention times, high energy requirements, membrane clogging, and associated additional chemical demands are different weaknesses of these processes (Bustillo-Lecompte & Mehrvar 2015; Moussa *et al.*, 2017; Shahediet *et al.*, 2020; Mousazadeh *et al.*, 2021). In biological processes, microorganisms are affected by toxic substances in the wastewater. In this context, nitrogen and phosphorus cannot be removed until satisfactory levels, requiring further treatment for safe discharge (Dadiet *et al.*, 2018; Musa *et al.*, 2021). The need to address water supply insecurity at both local and global levels, as well as the implementation of more rigorous laws, has increased the urgency of the advancement of wastewater treatment systems capable of processing and repurposing wastewater originating from poultry production enterprises (Avulaet *et al.*, 2009).

Heterogeneous photocatalysis (HPC) is one of the most promising AOPs. It is based on the generation of electron-hole pairs ( $e^-/h^+$ ) that catalyze organic pollutant degradation reactions (Silva *et al.*, 2007).  $\text{TiO}_2$ ,  $\text{ZnO}$ ,  $\text{CuO}$ ,  $\text{SnO}_2$ , and  $\text{CdS}$  are widely utilized semiconductors. Upon exposure to either natural or artificial radiation, these materials create holes in the valence band ( $h_{\text{VB}}^+$ ), electrons in the conduction band ( $e_{\text{CB}}^-$ ),  $\cdot\text{OH}$ , and superoxide radicals ( $\text{O}_2^{\cdot-}$ ) (Yeoh *et al.*, 2022). Ultrasound (US) or sonolysis is another innovative AOP based on the successful disintegration of microbubbles (encapsulated gas spheres of 0.1–10  $\mu\text{m}$  in diameter) through circular nucleation, propagation, and cavitation (Abdelhay *et al.*, 2020). Four major theories can explain sonochemical reactions: the hot-spot, plasma discharge, electrical,

and supercritical theories. According to the hot-spot theory, sonochemical reactions occur in three distinct zones in a homogeneous liquid: cavitation bubbles, the gas-liquid interface, and bulk solutions (Ozturk & Bal, 2015). AOPs have the capability of effectively treating a wide range of organic substances present in industrial wastewater, exhibiting high effectiveness rates (Davarnejad & Nasiri, 2017). US has the capability to break down hazardous organic substances into smaller molecules, also demonstrating a high level of effectiveness in the inactivation of microorganisms. (Abdelhay *et al.*, 2020).

Nevertheless, HPC and US still have some drawbacks, including a low mineralization of refractory contaminants, and a lower quantum yield due to a high charge recombination rate, respectively, while also incurring in high energy consumption, and high operating costs (Yeoh *et al.*, 2022). The combination of  $\text{H}_2\text{O}_2$ , US and HPC, called the sonophotocatalytic process (SPCP), is a type of hybrid AOP that increases pollutant removal efficiency, and is one of the most distinctive methods developed in recent years (Al-Bsoul *et al.*, 2020; Yang *et al.*, 2021; Dogdu & Sen, 2022). Its primary objective is the expansion of the physical effect of US by propagating it through the suspended catalyst particles, thereby preventing aggregation throughout the process (Panda & Manickam, 2017). The surface of the photocatalyst is also decontaminated by acoustic cavitation, thereby regenerating its active sites; and the catalyst surface serves as a location for cavitation bubble nucleation (Madhavan *et al.*, 2019). Consequently, this effect amplifies the increase in the quantity of  $\cdot\text{OH}$  produced through an increased surface area of the catalyst (Madhavan *et al.*, 2019; Al-Bsoul *et al.*, 2020; Dogdu & Sen, 2022).

To the authors' knowledge, no prior study has been done on the potential of using  $\text{H}_2\text{O}_2$  and US in conjunction with an HPC process for the treatment of PSW. In light of the above, the aim of this research was to design and implement a novel combined  $\text{H}_2\text{O}_2/\text{US}/\text{HPC}$  system for the removal of ammonia and phosphorus from PSW, and to determine the operational costs of this hybrid system as a whole. Furthermore, the Taguchi statistical design technique was used to improve, simplify, and standardize the experimental design, as well as to determine the optimal operating conditions with fewer experiments and at a lower cost, in order to obtain the highest nutrient removal from PSW based on the most efficient operating parameters (Besharati Fard *et al.*, 2020). An analysis of the operational cost of treating sectoral wastewater is another innovative contribution of this study.



## MATERIALS AND METHODS

### Chemicals

ZnO (99.9%, <5  $\mu\text{m}$  particle size, 10–25  $\text{m}^2/\text{g}$  BET surface area, Sigma-Aldrich),  $\text{TiO}_2$  (21 nm, AEROXIDE®  $\text{P}_{25}$   $\geq 99.5\%$ , anatase form, 35–65  $\text{m}^2/\text{g}$  BET surface area, Sigma-Aldrich), sodium hydroxide (NaOH, 99%, Merck),  $\text{H}_2\text{O}_2$  (30%, Sigma-Aldrich), and sulfuric acid ( $\text{H}_2\text{SO}_4$ , 97%, Merck) were used in this study. Deionized water (specific resistivity: 18.2  $\text{M}\Omega$ , Merck) was used to avoid ion interference during the preparation of all the solutions.

### Sample collection and analytical method

PSW samples were collected from a local chicken producer, located at Bolu, Turkey. Samples were collected from the effluent of the slaughterhouse, after offal screening, but prior to the facility's wastewater treatment plant. During the study period, composite samples were collected over a 24-hour period. These samples were collected in 5 L containers that were equipped with covers designed to prevent light exposure and leakage. The collection of these samples occurred on the first day of each week. The samples were subsequently transferred to the Bolu Abant Izzet Baysal University Wastewater Laboratory and stored at a constant temperature of 4°C in dark conditions before use. The facility processed 180,000 chickens with average weight of 2500 g, producing an average of 1,300–1,500  $\text{m}^3$  of wastewater per operating day. The physicochemical characteristics of raw and treated PSW were determined according to the Standard Methods for the Examination of Water and Wastewater methodology (APHA, 2017). The values of the physicochemical parameters of raw PSW are presented in Table 1. A pH meter (Orion Star A329 Thermo Scientific) was used for the assessment of pH. A turbidimeter (Sinsche TB2000) was used to measure PSW turbidity values (APHA 2530-B). The samples were centrifuged at 5000 rpm for 15 min (NUVE NF-200). Then, the supernatant was filtered through a 0.45  $\mu\text{m}$  filter (Minisart RC25, Sartorius).

COD was measured by using Merck Millipore® kits (APHA 5220-D) with a UV spectrophotometer (Spectroquant Pharo 100, Merck). A 3 mL sample was measured after treatment for 120 min at 150°C in the thermoreactor (Merck Spectroquant TR 320).

Biochemical oxygen demand was measured using a five-day BOD test (APHA, 2017-5210B). Total-N, total-P,  $\text{N}_4^+$ -N and  $\text{PO}_4$ -P levels were determined spectrophotometrically (Spectroquant Pharo 100, Merck) using Merck Millipore® kits. Averages for the three replications of each experimental analysis were calculated reported the study.

### Reactor set-up

The whole study was conducted using a double-walled reaction vessel and a pencil-type Pyrex glass immersion well photo-reactor equipped with a UVC<sub>254</sub> ultraviolet lamp (Philips, 9 W; 254 nm) or a PL-L UVA<sub>365</sub> lamp (Philips, 360 W; 315 to 380 nm; 110  $\text{W}/\text{cm}^2$ ), as illustrated in Figure 1.

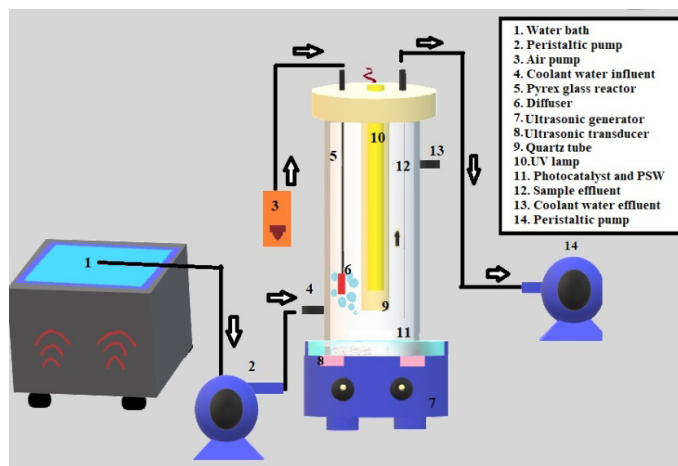


**Figure 1** – Scheme of experimental set-up for integrated SPCP.

A photo-reactor was installed in an ultrasonic bath tank (Bandelin DT 106) with a capacity of 5.6 L (operating volume, 200 mL). The tank dimensions were  $D = 240$  mm and  $L = 125$  mm, with an operating frequency of 35 kHz (120 W, 220 V), and an external generator (Dogdu & Sen, 2022; Dikmen *et al.*, 2022). A diffuser from which compressed air was bubbled into the solution maintained the air flow, and was adjusted to 3.5 L/min. Using a thermos state bath (NUVE ST-30) and a water circulation system (Filtec PH-15X3S-FPP-1), the interior temperature of the reactor was maintained at  $25 \pm 5^\circ\text{C}$  at all times.

### Experimental design and statistical analysis

The Taguchi method was applied to design experiments in the present study. Based on prior

**Table 1** – Main physicochemical characteristics of raw poultry slaughterhouse wastewater (No of samples=3).

Parameter	pH	Turbidity	COD	BOD5	TSS	T-N	T-P	NH <sub>4</sub> -N	PO <sub>4</sub> -P
Unit	-	NTU	mg/L	mg/L	mg/L	mg/L	mg/L	mg/L	mg/L
Value	7.37 ± 0.03	722 ± 2.52	3280 ± 39.1	2132 ± 492	493 ± 2.52	305 ± 5.00	247.7 ± 1.53	95 ± 5.00	105 ± 2.00



studies, it has been established that several key factors significantly influence the efficacy of system removal by different AOPs. These factors include pH levels, catalyst concentrations, catalyst types, UV lamp specifications, operation durations, and  $H_2O_2$  concentrations (Dogdu Okcu *et al.*, 2019; Dogdu & Sen, 2022; Dogdu, 2022).

Due to the limitations of the SPC reactor, changes in ultrasound frequency and power could not be investigated. Thus, the effects on AOPs of parameters such as UV lamp type (UVA<sub>365</sub>, UVC<sub>254</sub>), catalyst type (TiO<sub>2</sub>, ZnO), catalyst concentration (0.5, 1.5, 2.5 g/L), pH (2, 6, 10),  $H_2O_2$  dose (0, 5, 10 mmol/L), and time (30, 105, 180 min) were studied at the three levels presented in Table 2.

**Table 2** – Operating parameters and design levels of the Taguchi orthogonal array.

Parameters	Labels	Levels		
		L <sub>1</sub>	L <sub>2</sub>	L <sub>3</sub>
Catalyst type	CT	TiO <sub>2</sub>	ZnO	
UV lamp type	LT	UVA <sub>365</sub>	UVC <sub>254</sub>	
Catalyst dosage (g/L)	CC	0.5	1.5	2.5
pH	pH	2	6	10
$H_2O_2$ concentration (mmol/L)	C <sub>H<sub>2</sub>O<sub>2</sub></sub>	0	5	10
Operation time (min)	t	30	105	180

The Taguchi L<sub>36</sub> (2<sup>2</sup> × 3<sup>4</sup>) orthogonal array (three repetitions at each experiment) was conducted with Minitab 17.0 Statistical Software to optimize the operating parameters and statistical analysis based on ANOVA and S/N ratio, as shown in Table 3. N<sub>4</sub><sup>+</sup>-N and PO<sub>4</sub>-P removal yields are the evaluated response variables. SigmaPlot 12 was used to produce graphs for the paper. The output signal-to-noise ratio (S/N), which depends on the optimization criterion for the response variable, is a statistical measure of the Taguchi method's process efficacy (Sousa *et al.*, 2020). "Larger-the-better" criteria were chosen for the S/N ratio according to the type of optimization (Besharati Fard *et al.*, 2020). In the current investigation, the system underwent optimization with the objective of maximizing N<sub>4</sub><sup>+</sup>-N and PO<sub>4</sub>-P-removal yields.

## RESULTS AND DISCUSSION

### Preliminary studies

The effluent characteristics of raw PSW are given in Table 1. Figure 2 shows the percentages of N<sub>4</sub><sup>+</sup>-N and PO<sub>4</sub>-P removal from PSW after a 180-min working period of different single AOPs, namely catalysis (TiO<sub>2</sub>, ZnO), sonolysis (US), photolysis (P) (UVA<sub>365</sub>, UVC<sub>254</sub>), and H<sub>2</sub>O<sub>2</sub>, as determined by preliminary studies. All procedures were undertaken under the same operating

conditions. N<sub>4</sub><sup>+</sup>-N removal efficiencies with single AOPs were 17±0.95%, 9±0.52%, 18±0.52%, 9±0.52%, 10±0.6%, and 19±0.50% for US, UVA<sub>365</sub>, UVC<sub>254</sub>, TiO<sub>2</sub>, ZnO, and H<sub>2</sub>O<sub>2</sub>, respectively; while PO<sub>4</sub>-P removal efficiencies were respectively 17±0.64%, 2.2±0.2%, 6±0.64%, 7±0.36%, and 3±0.50%. As shown in Figure 2 and Table 4, integrated energy-based AOPs yielded N<sub>4</sub><sup>+</sup>-N removal efficiencies between 20 and 52%, while PO<sub>4</sub>-P removal efficiencies ranged from 22 to 60%. Based on the results, the removal efficiency of nutrients from PSW is greater for hybrid processes that implement multiple AOPs than for single processes.

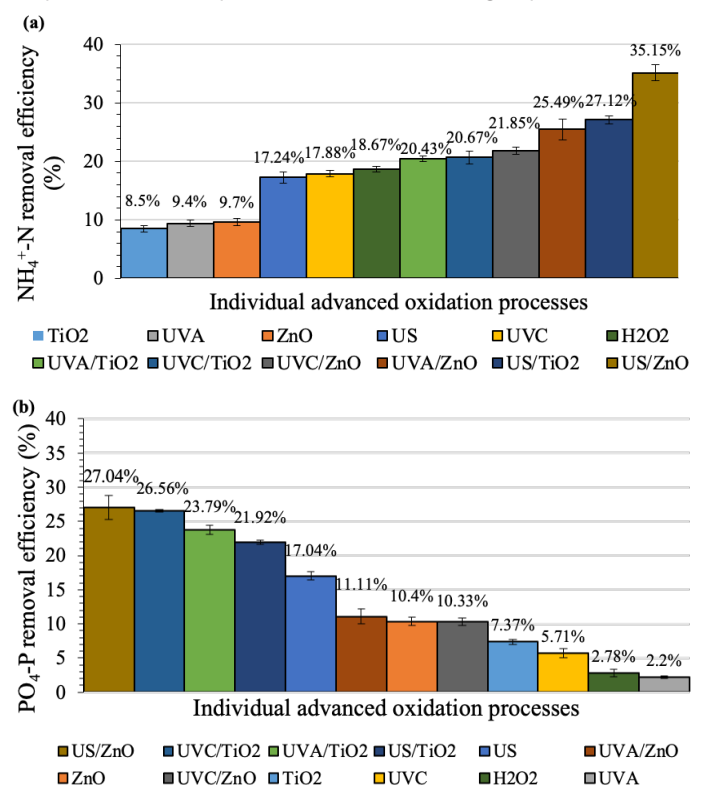


**Figure 2** – Individual and integrated AOP removal yields for (a) NH<sub>4</sub><sup>+</sup>-N and (b) PO<sub>4</sub>-P in PSW (operating conditions: US frequency: 35 kHz; US power: 120W; pH: 6; CC: 1.5 g/L; C<sub>H<sub>2</sub>O<sub>2</sub></sub>: 10 mmol/L; UV power: 36W; t: 180 minutes; T: 25±2 °C).

Furthermore, the earlier study conducted by Dogdu & Sen (2022) reported that the hybrid H<sub>2</sub>O<sub>2</sub>/US/HPC process achieved a COD removal of 54% and oil & grease (O&G) removal of 99% after a process duration of 180 min. As shown in Table 1, the data revealed that, after offal screening, the slaughterhouse unit effluent was characterized by a high organic matter load. The COD/BOD<sub>5</sub> ratio was also calculated to assess the potential biodegradability of the organic contents in the PSW. An increased COD/BOD<sub>5</sub> ratio indicates a higher proportion of slow biodegradable and non-biodegradable compounds in the sample. In the case of biodegradable organics, COD is normally within the range of 1.3 to 1.5 times the BOD. When the result



**Table 3** – Signal-to-noise ratio (S/N) data on responses for overall response variables (CT: catalyst type, LT: lamp type, CC: catalyst dosage, CH<sub>2</sub>O<sub>2</sub>: Hydrogen peroxide concentration, t: time).

NH <sub>4</sub> <sup>+</sup> -N removal (%)							PO <sub>4</sub> -P removal (%)						
Level	CT	LT	CC (g/L)	pH	C <sub>H<sub>2</sub>O<sub>2</sub></sub> (mmol/L)	t (min)	Level	CT	LT	CC (g/L)	pH	C <sub>H<sub>2</sub>O<sub>2</sub></sub> (mmol/L)	t (min)
1	19.35	22.45	23.46	21.09	23.84	20.62	1	22.84	23.1	17.17	29.61	20.53	19.15
2	26.14	23.56	19.95	16.88	21.31	28.15	2	21.3	22.75	27.27	16.7	23.53	26.16
3			25.74	31.19	24.01	20.38	3			24.28	22.4	24.66	23.4
Delta	6.8	1.11	5.78	14.3	2.7	7.77	Delta	3.54	0.35	10.1	12.91	4.13	7.01
Rank	3	6	4	1	5	2	Rank	5	6	2	1	4	3

of a COD test is more than twice that of the BOD test, there is good reason to suspect that a significant portion of the organic material in the sample is not biodegradable by ordinary microorganisms (Woodard, 2001). The COD/BOD<sub>5</sub> ratio in the wastewater from the slaughterhouse unit is approximately 1.54. In other words, the BOD<sub>5</sub>/COD ratio was about 0.65, indicating that 65% of the COD of this wastewater could easily be degraded by biological treatment (Bazrafshan *et al.*, 2012). However, the remaining COD was high, indicating the need for an effective physicochemical treatment. The maximum COD removal of 54% by the hybrid H<sub>2</sub>O<sub>2</sub>/US/HPC process showed that this method can be an effective pretreatment method for wastewater such as PSW.

Based on the data, it is hypothesized that the enhanced efficacy in nutrient removal observed in the hybrid H<sub>2</sub>O<sub>2</sub>/US/HPC system, as opposed to single AOPs, can be attributed to the combined degradation of nonbiodegradable and refractory chemicals present in the PSW by combining US, H<sub>2</sub>O<sub>2</sub>, photocatalyst and UV irradiation. Furthermore, the results of an earlier study showed that US enabled the breakdown of O&G in addition to the oxidation and destruction of aromatic compounds in PSW caused by the presence of a photocatalyst, H<sub>2</sub>O<sub>2</sub>, and UV irradiation (Dogdu & Sen, 2022). Thus, 99% O&G and color removal could be achieved in 180 min. Nevertheless, despite 180-min being sufficient to achieve maximum degradation of COD, NH<sub>4</sub><sup>+</sup>-N, and PO<sub>4</sub>-P, the average removal efficiency of these parameters, ranging from 50% to 60%, might be attributed to the accumulation of high concentrations of intermediate products. These intermediates are unable to undergo further oxidation by OH· due to the hybrid AOP process and thus accumulate in the system (Al-Bsoul *et al.*, 2020). Moreover, real wastewater typically contains a variety of contaminants instead of just one type, which is often the main focus of research. Hence, it can be inferred that the presence of various contaminants will complicate the process of sonophotocatalytic degradation in intricate ways (Mapukata *et al.*, 2023).

### Taguchi design and statistical analysis

Table 4 presents the results of 36 experiments on NH<sub>4</sub><sup>+</sup>-N and PO<sub>4</sub>-P removals from PSW. In order to optimize the nutrient removal process, the output S/N ratio from the Taguchi method was used to identify the distinguishing characteristics between signal factors and the control, considered that “larger is better” for each test run. Table 4 shows that NH<sub>4</sub><sup>+</sup>-N removal efficiencies range between 2% and 52%, whereas PO<sub>4</sub>-P removal efficiencies vary between 2% and 60%. The S/N ratios are displayed in Table 3 and Figure 3, demonstrating the independent process components (CC, CT, LT, pH, C<sub>H<sub>2</sub>O<sub>2</sub></sub>, and t) that yield the highest levels of NH<sub>4</sub><sup>+</sup>-N and PO<sub>4</sub>-P removal efficiency.

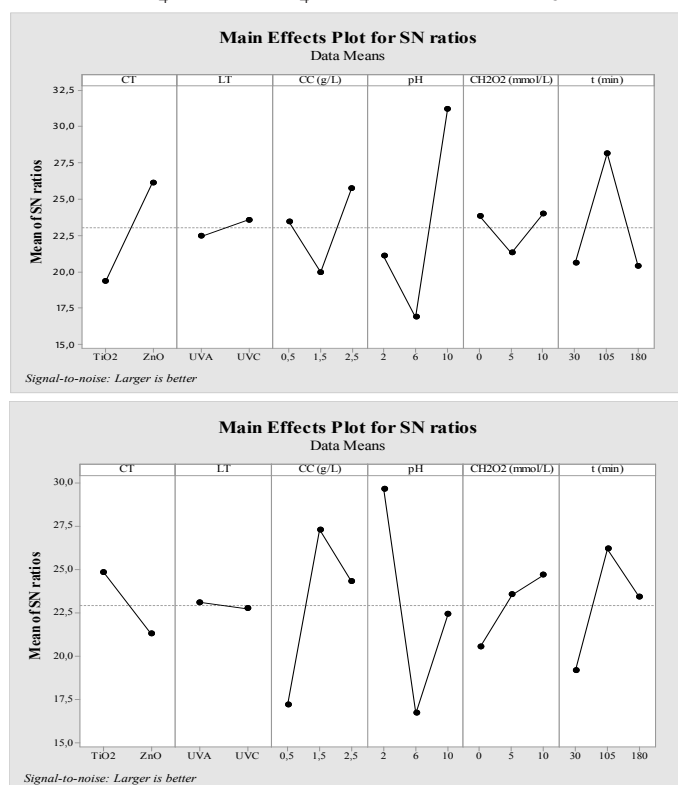


**Figure 3** – Principal influences of S/N parameters on (a) NH<sub>4</sub><sup>+</sup>-N and (b) PO<sub>4</sub>-P removal efficiencies (CT: catalyst type, LT: lamp type, CC: catalyst dosage, C<sub>H<sub>2</sub>O<sub>2</sub></sub>: Hydrogen peroxide concentration, t: time).

The results of the analysis of variance (ANOVA) demonstrating the influence of control factors on the



**Table 4** – Experimental results of the Taguchi method's  $\text{NH}_4^+\text{-N}$  and  $\text{PO}_4\text{-P}$  removal efficiencies (CT: catalyst type, LT: lamp type, CC: catalyst dosage,  $C_{\text{H}_2\text{O}_2}$ : Hydrogen peroxide concentration, t: time).

Parameters							$\text{NH}_4^+\text{-N}$ removal		$\text{PO}_4\text{-P}$ removal	
No.	CT	LT	pH	CC (g/L)	$C_{\text{H}_2\text{O}_2}$ (mmol/L)	t (min)	S/N (dB)	Percentage (%)	S/N (dB)	Percentage (%)
1	TiO <sub>2</sub>	UVA	2	0.5	0	30	15.11	7.14	21.71	11.28
2	TiO <sub>2</sub>	UVA	6	1.5	5	105	7.13	2.33	27.82	26.65
3	TiO <sub>2</sub>	UVA	10	2.5	10	180	31.84	37.50	31.43	38.68
4	TiO <sub>2</sub>	UVA	2	0.5	0	30	15.11	4.88	21.71	13.33
5	TiO <sub>2</sub>	UVA	6	1.5	5	105	7.13	2.22	27.82	22.96
6	TiO <sub>2</sub>	UVA	10	2.5	10	180	31.84	40.91	31.43	36.03
7	TiO <sub>2</sub>	UVA	2	0.5	5	180	5.51	1.89	17.86	7.81
8	TiO <sub>2</sub>	UVA	6	1.5	10	30	5.68	1.92	26.47	21.05
9	TiO <sub>2</sub>	UVA	10	2.5	0	105	32.51	42.20	29.15	28.68
10	TiO <sub>2</sub>	UVC	2	0.5	10	105	30.31	32.77	22.50	13.33
11	TiO <sub>2</sub>	UVC	6	1.5	0	180	5.51	1.89	8.63	2.70
12	TiO <sub>2</sub>	UVC	10	2.5	5	30	28.06	25.29	28.20	25.71
13	TiO <sub>2</sub>	UVC	6	0.5	10	30	6.02	2.00	11.12	3.60
14	TiO <sub>2</sub>	UVC	10	1.5	0	105	32.20	40.74	29.15	28.68
15	TiO <sub>2</sub>	UVC	2	2.5	5	180	18.24	8.16	30.39	33.07
16	TiO <sub>2</sub>	UVC	6	0.5	10	105	26.00	19.96	25.95	19.85
17	TiO <sub>2</sub>	UVC	10	1.5	0	180	27.31	23.20	30.27	32.62
18	TiO <sub>2</sub>	UVC	2	2.5	5	30	18.74	8.65	31.90	39.33
19	ZnO	UVA	6	0.5	0	180	20.92	11.11	26.37	20.83
20	ZnO	UVA	10	1.5	5	30	26.50	21.13	22.67	13.61
21	ZnO	UVA	2	2.5	10	105	29.95	31.45	33.62	48.00
22	ZnO	UVA	6	0.5	5	180	20.60	10.71	8.87	2.78
23	ZnO	UVA	10	1.5	10	30	31.00	35.48	21.09	11.33
24	ZnO	UVA	2	2.5	0	105	29.95	31.44	33.87	49.40
25	ZnO	UVA	10	0.5	5	30	31.65	38.24	5.96	1.99
26	ZnO	UVA	2	1.5	10	105	26.74	21.74	31.75	38.70
27	ZnO	UVA	6	2.5	0	180	21.58	12.00	7.82	2.46
28	ZnO	UVC	10	0.5	5	105	33.62	48.00	18.70	8.61
29	ZnO	UVC	2	1.5	10	180	21.24	11.54	34.84	55.19
30	ZnO	UVC	6	2.5	0	30	24.08	16.00	2.73	1.37
31	ZnO	UVC	10	0.5	10	180	34.03	50.30	25.51	18.87
32	ZnO	UVC	2	1.5	0	30	18.79	8.70	31.83	39.02
33	ZnO	UVC	6	2.5	5	105	26.94	22.22	30.96	35.33
34	ZnO	UVC	10	0.5	0	105	34.32	52.00	4.29	1.64
35	ZnO	UVC	2	1.5	5	180	17.39	7.41	35.46	59.50
36	ZnO	UVC	6	2.5	10	30	21.24	11.54	7.00	2.24

removal of nutrients from PSW are also presented in Table 5, at a significance level of  $\alpha = 0.05$  and a level of confidence of 95%. As shown in Table 5, the errors for  $\text{NH}_4^+\text{-N}$  and  $\text{PO}_4\text{-P}$  removal were 4% and 32%, respectively, well below the limit value (50%); thus, the experimental errors are insignificant.

The contribution percentage ( $C_r$  %) is used for quantitative evaluation and is presented in Table 5. According to the obtained percentage contribution values, the most influential parameters on the  $\text{NH}_4^+\text{-N}$  removal efficiency were pH (F: 217.71,  $C_r$ : 63.31%), operation time (F: 50.41,  $C_r$ : 14.46%), catalyst concentration (F: 24.29,  $C_r$ : 7.06%), catalyst type (F: 41.46,  $C_r$ : 6.03%), and  $\text{H}_2\text{O}_2$  concentration (F: 16.82,

$C_r$ : 4.89%). Furthermore, the most influential factors affecting the efficiency of  $\text{PO}_4\text{-P}$  removal were catalyst concentration (F: 10.92,  $C_r$ : 28.24%), pH (F: 10.34,  $C_r$ : 26.65%), and operation time (F: 3.88,  $C_r$ : 10.04%).

The steepest inclination of the pH line is depicted in Figure 3(a), which demonstrates an excessively significant influence of this variable on  $\text{NH}_4^+\text{-N}$  removal ( $p < \alpha$ ,  $\alpha = 0.05$ ). The following parameters were significant ( $p < \alpha$ ,  $\alpha = 0.05$ ): CC, CT,  $C_{\text{H}_2\text{O}_2}$ , and t. Furthermore, Figure 3(b) demonstrates that catalyst concentration and pH exhibited the steepest inclinations, indicating their utmost significance for  $\text{PO}_4\text{-P}$  removal ( $p < \alpha$ ,  $\alpha = 0.05$ ). Operation time is also a significant factor in the removal of  $\text{PO}_4\text{-P}$  ( $p < \alpha$ ,



**Table 5** – Obtaining ANOVA results for the removal efficiency of (a)  $\text{NH}_4^+\text{-N}$  and (b)  $\text{PO}_4\text{-P}$  ( $C_T$ : catalyst type,  $L_T$ : lamp type,  $C_C$ : catalyst dosage,  $C_{\text{H}_2\text{O}_2}$ : Hydrogen peroxide concentration,  $t$ : time).

Source	Sum of squares	Degree of freedom	Mean square	F value	p value	Contribution (%)
<b><math>\text{NH}_4^+\text{-N}</math> removal (%)</b>						
$C_T$	524.09	1	524.09	41.46	0.000	6.03
$L_T$	36.14	1	36.14	2.86	0.103	0.42
$C_C$	614.11	2	307.05	24.29	0.000	7.06
pH	5503.71	2	2751.9	217.71	0.000	63.31
$C_{\text{H}_2\text{O}_2}$	425.09	2	212.54	16.82	0.000	4.89
$t$	1274.41	2	637.21	50.41	0.000	14.66
Error	316	25	12.64			3.63
Lack of-Fit	307.62	22	13.98	5.01	0.105	3.54
Pure Error	8.38	3	2.79			0.1
Total	8693.54	35				100
$R^2=0.9637$		$R^2_{(\text{pred})}=0.9491$		$R^2_{(\text{adj})}=0.9246$		
Source	Sum of squares	Degree of freedom	Mean square	F value	p value	Contribution (%)
<b><math>\text{PO}_4\text{-P}</math> removal (%)</b>						
$C_T$	0.77	1	0.77	0.01	0.938	0.01
$L_T$	17.21	1	17.21	0.14	0.715	0.18
$C_C$	2747.11	2	1373.55	10.92	0.000	28.24
pH	2602.09	2	1301.05	10.34	0.001	26.75
$C_{\text{H}_2\text{O}_2}$	236.82	2	118.41	0.94	0.404	2.43
$t$	976.55	2	488.28	3.88	0.034	10.04
Error	3145.46	25	125.82			32.34
Lack of-Fit	3133.04	22	142.41	34.4	0.007	32.21
Pure Error	12.42	3	4.14			0.13
Total	9726.01	35				100
$R^2=0.6766$		$R^2_{(\text{pred})}=0.5472$		$R^2_{(\text{adj})}=0.3294$		

$\alpha=0.05$ ). Lamp type is not statistically significant for the removal of either pollutant ( $p>\alpha$ ,  $\alpha=0.05$ ). The optimal combination of operating parameters to maximize the S/N ratio and, consequently, the  $\text{NH}_4^+\text{-N}$  removal efficiency of the  $\text{H}_2\text{O}_2/\text{US}/\text{HPC}$  hybrid was as follows: catalyst type level 2 (ZnO), catalyst concentration level 3 (2.5 g/L), lamp type level 2 (UVC<sub>254</sub>), pH level 3 (pH 10),  $\text{H}_2\text{O}_2$  dose level 3 (10 mmol/L), and reaction time level 2 (105 min). Moreover, the optimal operating parameter combination for  $\text{PO}_4\text{-P}$  removal efficiency was found to be catalyst type level 1 ( $\text{TiO}_2$ ), catalyst concentration level 2 (1.5 g/L), lamp type level 1 (UVA<sub>365</sub>), pH level 1 (pH 2),  $\text{H}_2\text{O}_2$  dosage level 3 (10 mmol/L), and reaction time level 2 (105 min). In addition, lamp type was found to be statistically insignificant for the removal of either nutrient from PSW ( $p>\alpha$ ,  $\alpha=0.05$ ). Even though the wastewater and reactor configuration used in the study were identical, the results showed that optimal operating conditions varied depending on each pollutant parameter. Since the reaction time to attain maximum nutrient removal is the same for both parameters (105 min), the system can be optimized based on either parameter.

## Ammonia removal

Figure 2(a) illustrates that US alone exhibited an efficacy of only 18% in the removal of ammonium-N. The ammonium-N removal efficacy was found to be 9–17% when a catalyst (either  $\text{TiO}_2$  or ZnO) was present. Conversely, when solely UV irradiation (either UV-A or UV-C) was used, the average ammonium-N removal efficiency was 10%. Throughout the HPC studies, a diffuser with a 3.5 L/min air flow was used to aerate the whole reactor system. Ammonium-N removal efficiency in the presence of UV irradiation and a photocatalyst is shown in Figure 2(a) to be 25%, on average. In the presence of only  $\text{H}_2\text{O}_2$ , ammonium-N removal efficiency is 19%. In this case, while an ammonium-N removal efficiency averaging around 20% can be achieved with individual AOPs, as seen in Table 4, the use of a hybrid  $\text{H}_2\text{O}_2/\text{US}/\text{HPC}$  treatment increased synergistic effects and led to an efficiency above 50%. In addition to enhancing the rate of mass transfer, US could influence chemical reactions by generating enormous heat (pyrolysis) or reactive free radicals (Suslick, 1989).



There is a significant association between the deterioration of ammonia and the state of ammonia in a solution containing water (Wu *et al.*, 2019). Ammonia has the ability to exist in two forms:  $\text{NH}_3$  gas, often known as volatile free ammonia, or ammonium ion ( $\text{NH}_4^+$ ) dissolved in an aqueous solution. The form it takes is determined by the pH of the surrounding environment (Gay and Knowlton, 2005). According to the data shown in Table 5(a), it can be observed that the pH parameter exhibits the highest contribution of 63% towards the elimination of ammonia. The concentration of ammonia in the molecular state exhibits an upward trend as the pH level increases. During the process of bubbling, it is observed that ammonium ions display a lack of vaporization, whereas ammonia, on the other hand, can be vaporized. According to previous studies (Wang *et al.*, 2008; Sivasankar and Moholkar, 2009), it is expected that the prevailing ammonia species will volatilize and then undergo pyrolysis under elevated pH values. Nevertheless, it is worth noting that decreased pH levels can lead to a prevalence of ammonium ions within the solutions. Therefore, it is not expected that ammonium ions will distribute within the bubble, and the only anticipated breakdown mechanism is hydroxylation.

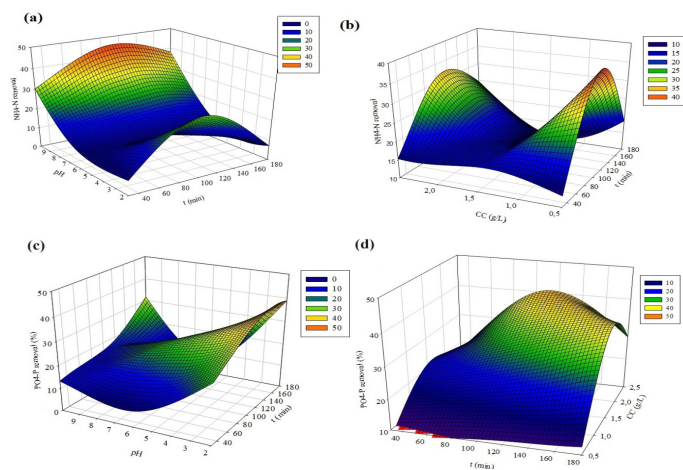


**Figure 4** – Effects of (a) pH and (b) photocatalyst concentration on ammonium-N removal; effects of (c) pH and (d) photocatalyst concentration on phosphorus removal (CC: catalyst dosage, and t: time).

As depicted in Figure 3(a) and Figure 4(a), concerning the pH change phenomenon investigated in the aforementioned prior research, it is thought that up to pH 6, ammonia is dominated by ammonium ions and radical oxidation is the primary pathway for ammonia degradation. Purwonoet *al.* (2017) investigated total ammonia removal from domestic wastewater and reported that the total ammonia removal procedure reduced  $\text{NH}_4^+$ -N and produced  $\text{NH}_3$ -N, but the  $\text{NH}_3$ -N level could increase due to a pH increase. When the

pH is increased to 10, the concentration of ammonium ions and the decomposition of ammonia by radical oxidation both decrease. US improve the removal efficiency of free volatile ammonia as the pH increases (Yu *et al.*, 2021). Wang *et al.* (2008) and Xu *et al.* (2005) declared that the optimal pH range for ammonia-N removal was between 8 and 11. Consequently, as depicted in Figure 4(a), it is believed that the quantity of ammonia that can be removed increases as the pH increases from 6 to 10. This is likely due to the fact that US eliminates more free volatile ammonia and radical oxidation eliminates more ammonium ions.

Furthermore, it is widely recognized that the utilization of ultrasonic and cavitation techniques lead to the generation of highly vigorous micro-mixing phenomena. This enhanced micro-mixing facilitates a heightened level of interaction between contaminants and the radicals that are formed as a result of cavitation bubble formation (Ozturk & Bal, 2015). In this study, the use of  $\text{H}_2\text{O}_2$  in addition to US and HPC also contributed to radical formation. Therefore, it can be inferred that removal performances are influenced by the interacting effects of physical and chemical factors. Hence, based on the pH trend observed in Table 2 of this research, it is hypothesized that the elimination of volatile ammonia is enhanced due to the interaction between the radicals generated by the cavitation bubbles and the ammonia present in the PSW, facilitated by the assistive mechanisms described earlier, namely US. Xu *et al.* (2005) discussed the impact of initial pH levels on the elimination of ammonia-nitrogen from coke plant effluent through the application of ultrasonic irradiation. The experiment involved subjecting samples with an initial concentration of 121 mg/l ammonia to sonication for duration of 240 min within a pH range of 3–7. Maximum ammonia removal efficiency was reached between pH 8.2 and 11, with removal efficiency exceeding 55%. García-Prieto *et al.* (2022) investigated the degradation of  $\text{NH}_4^+/\text{NH}_3$  in aqueous media using a pilot-scale photoreactor with heterogeneous photocatalysis ( $\text{TiO}_2/\text{SiO}_2$ ) and photolysis under UVC irradiation, yielding results comparable to those of this investigation. The greatest level of degradation was observed at the highest pH investigated (pH 11) and with the use of a higher lamp irradiation power (25 W), resulting in 44.1% (photolysis) and 59.1% (photocatalysis) degradation efficiencies.

The operating time is identified as an additional significant factor influencing the efficiency of ammonium-N removal, being responsible for a 15%



contribution, according to the ANOVA results provided in Table 5. As presented in Figure 3(a), ammonium-N removal increases rapidly from the 30<sup>th</sup> to 105<sup>th</sup> min, after which it undergoes a pronounced decline until the 180 minutes mark. The observed phenomenon is believed to be a result of the gradual reduction in ammonia concentration over time, as well as the diminishing opportunity for interaction with  $\cdot\text{OH}$  and superoxide radicals ( $\cdot\text{O}_2^-$ ) inside the aqueous solution. In sonication studies, it has been observed that the quantity of cavitation bubbles and the levels of sonic energy imparted to the solution exhibit an upward trend with increasing sonication time. However, it is worth noting that the most effective removal of ammonia is attained over a relatively short period of sonication (Ozturk & Bal, 2015). Gong *et al.* (2015) declared that photocatalytic degradation of ammonia results in the formation of a significant number of intermediates that cannot be removed efficiently in the reactor. Similarly, in the present study, intermediate products formed due to the photocatalytic degradation of pollutants in PSW may have accumulated and deposited on the photocatalyst film surfaces around the reaction time of 105 min, gradually deactivating the active sites and reducing the formation of hydroxyl radicals and active oxygen species, which play an important role in oxidation on the thin film surface. The decrease in ammonium-N removal yield in the hybrid  $\text{H}_2\text{O}_2/\text{US}/\text{HPC}$  process depends on the formation of intermediates when the reaction period is extended to 180 min, as depicted in Figure 3(a).

As shown in Table 4, catalyst concentration at a level of 7% is the third most influential factor in the ammonium-N removal process. Figure 3(a) and Figure 4(b) illustrate that an increase in catalyst concentration from 0.5 to 1.5 g/L decreased ammonium-N removal. The ammonium-N concentration in the raw PSW introduced in the reactor system is notably high, varying between 90 and 100 mg/L. Therefore, it is likely that the surface of the photocatalyst underwent a significant ammonium coating, especially in the early stages of the process when ammonium ions were abundant and radical oxidation was expected to occur. This coating may hinder the excitation of photogenerated electron-hole pairs and the subsequent generation of  $\cdot\text{OH}$  and  $\cdot\text{O}_2^-$ , thereby diminishing the efficiency of ammonium nitrogen removal (Wang *et al.*, 2008; Yu *et al.*, 2021).

$\text{TiO}_2$  and  $\text{ZnO}$  photocatalysts were used to study the effect of photocatalyst type on ammonium-N removal. During the preliminary adsorption investigations,  $\text{ZnO}$  and  $\text{TiO}_2$  exhibited comparable (10% and 9%,

respectively) ammonium-N removal capacities, as shown in Figure 2(a). Nevertheless, according to Table 5, the effect of the catalyst type on ammonium-N removal in the integrated  $\text{H}_2\text{O}_2/\text{US}/\text{HPC}$  was statistically significant, accounting for approximately 6% of the total effect. Despite having similar band gaps of 3.2 eV and 3.3 eV (for  $\text{TiO}_2$  and  $\text{ZnO}$ , respectively), as well as favorable chemical and optical stability, and impressive environmental and biological compatibility, their notable drawback lies in their limited sensitivity to visible light. Additionally, the rapid recombination rate of electron-hole pairs generated by irradiation was identified as a drawback for  $\text{TiO}_2$ , whereas  $\text{ZnO}$  exhibited enhanced solubility in water under the influence of UV light (Chakhtouna *et al.*, 2021; Hernández *et al.*, 2015). Table 3 demonstrates that  $\text{ZnO}$  was superior to ammonium-N removal via sonophotocatalysis in the current study. Similarly, Jandaghian *et al.* (2023) reported that, under UV irradiation, the removal of levofloxacin by adsorption by  $\text{TiO}_2$  and  $\text{ZnO}$  sharply increased to approximately 67% and 86%, respectively, and that the higher photocatalytic degradation with  $\text{ZnO}$  is attributed to the higher electron mobility of  $\text{ZnO}$  (200–300  $\text{cm}^2/\text{Vs}$ ) in comparison to  $\text{TiO}_2$  (0.1–0.4  $\text{cm}^2/\text{Vs}$ ). Also, the valance band of  $\text{ZnO}$  ( $\text{VB}_{\text{ZnO}}$ ) exhibits a comparatively lower position compared to the valance band of  $\text{TiO}_2$  ( $\text{VB}_{\text{TiO}_2}$ ), resulting in a greater oxidation potential of the hydroxyl radical generated by  $\text{ZnO}$  in comparison to the hydroxyl radical produced by  $\text{TiO}_2$ . Consequently, this disparity contributes to an enhanced photocatalytic performance (Turkten & Bekbolet, 2020).

$\text{H}_2\text{O}_2$  is a potent oxidizing agent that enhances the photocatalyst's production of  $\cdot\text{OH}$  and  $\cdot\text{O}_2^-$ , and enhances its photocatalytic activity (Yu *et al.*, 2021). The introduction of  $\text{H}_2\text{O}_2$  has the capability to produce oxygen through its inherent breakdown reaction, particularly in alkaline conditions (Wenjun *et al.*, 2012). If the solution reaches a state of saturation with oxygen, it is conceivable that the dissolved oxygen could act as nucleation sites for the occurrence of sonic cavitation. Additionally, the gas phase can generate peroxy and hydroxyl radicals through the breakdown of molecular oxygen (Wenjun *et al.*, 2012). The recombination of these radicals at cooler locations, such as the interface or solution bulk, leads to the production of extra  $\text{H}_2\text{O}_2$  (Li *et al.*, 2012). Based on the data presented in Table 5, it can be concluded that the effect of  $\text{H}_2\text{O}_2$  concentration on ammonium-N removal is statistically significant. However, it is important to note that  $\text{H}_2\text{O}_2$  concentration contributes only 5% to ammonium-N



removal. Upon analysis of the signal-to-noise (S/N) data pertaining to the concentration of  $H_2O_2$  presented in Table 3, it can be seen that a change of only 0.71% occurred when the  $H_2O_2$  concentration increased from 0 to 10 mmol/L. In contrast, a difference of 11% was observed when the concentration was increased from 5 to 10 mmol/L. The prevalence of the ammonium ion at pH levels below 6 indicates that radical oxidation can be an effective technique for the efficient degradation of ammonia. Consequently, an increase in  $H_2O_2$  concentration from 0 to 5 mmol/L reduces ammonia removal, possibly due to a scavenging effect caused by the reaction of excess  $H_2O_2$  with HO (Patidar and Srivastava, 2021). When the pH rises above 6, the primary mechanism for the elimination of free volatile ammonia via ultrasound is revealed.

### Phosphorus removal

As depicted in Figure 3(b),  $PO_4$ -P removal with only US processing was of 17%, while the HPC process efficiency was about 10–27% and US efficiency was around 22–27%. In Table 4,  $PO_4$ -P removal with the  $H_2O_2$ /US/HPC hybrid increased to a maximum of 60%. The primary factor contributing to the observed increase in yield in the  $H_2O_2$ , US, and HPC process was the enhanced production of active species and the facilitation of mass transfer between the liquid phase and the surface of the photocatalyst. This is attributed to the generation of a larger quantity of cavitation bubbles through ultrasound, and a greater number of radicals resulting from the separation of electron-hole pairs in semiconductor photocatalysts (Wang & Cheng, 2023).

The pH parameter significantly contributes 26% to the removal of phosphorus during the  $H_2O_2$ , US, and HPC process, as presented in Table 5. Figure 3(b) and Figure 4(c), demonstrate that the most significant phosphorus removal occurred at a pH level of 2. However, as the pH level increased to 6, phosphorus removal gradually decreased. The relationship between pH and phosphorus adsorption can be elucidated using the pH function (Kang *et al.*, 2011). Choi *et al.* (2016) stated that pH levels influence the removal of phosphorus. In particular, it was observed that  $H_2PO_4^-$  is the predominant species in pH ranges between 4 and 7, while  $HPO_4^{2-}$  becomes the dominant species in pH ranges between 7 and 10. Consequently, the presence of different phosphorus species will influence the adsorption behavior of the photocatalyst onto the surface of the particle. It is widely recognized that certain particular phenomena occur when pH reaches

values above the point of zero charge (PZC) of titania, which has been experimentally determined to be 6.25 in the case of  $P_{25}$  (Conte *et al.*, 2021). The pH at which the discharge of  $TiO_2$  reaches the point of zero charge ( $pH_{zpc}$ ) is characterized by a positive electrical charge. Conversely, a negative charge is observed on the surface of  $TiO_2$  above the  $pH_{zpc}$ . Neutral groups predominate on the surface of  $TiO_2$  particles close to the  $pH_{zpc}$ , while charged species such as  $O^-$  and  $OH_2^+$  are negligible. It is expected that in an environment with low pH, there will be a tendency for adsorption to occur as a result of the attractive forces between the surface of  $TiO_2$  and negatively charged chemicals, including anions such as chloride ( $Cl^-$ ), phosphate ( $PO_4^{3-}$ ), and other similar substances. The possible hindrance of  $OH^-$  ion formation and the obstruction of substrate access to active surface sites may lead to a decrease in photocatalytic activity, which can be attributed to the existence of specific anions. Furthermore, the surface of  $TiO_2$  exhibits a negative charge, leading to repulsive interactions that can result in reduced adsorption at higher pH values (Cho *et al.*, 2002).

In any degradation process, catalyst concentration is regarded as one of the most crucial parameters from an economic standpoint. Table 5 demonstrates that catalyst concentration contributes the most to phosphorus removal at 28%. As shown in Figure 2(b), phosphorus removal based on the adsorption process with photocatalysts alone was 7–10%, whereas UV irradiation increased phosphorus removal efficiency up to 25%. The utilization of nanoparticles such as  $TiO_2$  and ZnO in this research is due to their capacity for phosphorus adsorption. Consequently, these nanoparticles serve a dual purpose as catalysts and sorbents, facilitating the efficient removal of phosphorus from wastewater through physical adsorption at elevated concentrations (Mayer *et al.*, 2016). Additionally, the study suggests that the removal of 7–10% of RP and nRP was probably accomplished solely through adsorption by catalysts in a dark environment without the use of ultrasonic treatment.

The adsorption of phosphorus is enhanced by the positively charged surface of titanium oxides, such as  $TiOH_2^+$ . The phenomenon of electrostatic attraction between  $TiOH_2^+$  and phosphate ions must be considered in relation to the process of adsorption (Moharami & Jalali, 2014). UV oxidation facilitates the release of RP from the catalyst surface while also promoting the conversion of a portion of the nRP present in the effluent to RP. Subsequently, through the involvement



of US, a greater quantity of orthophosphate and intermediate compounds are believed to be extracted from the solution, leading to the belief that the phosphorus removal efficiency of  $H_2O_2$ , US, and HPC can potentially reach a level of 60%.

Gray *et al.* (2020) stated that only 35 g phosphorus per liter (P/L) of a synthetic industrial wastewater sample with a concentration of 1900 g P/L contained reactive phosphorus (RP), while the majority of the phosphorus present was non-reactive phosphorus (nRP). Accordingly, it is believed that adsorption is predominantly responsible for a significant amount of the phosphorus that is eliminated following the introduction of a  $TiO_2$  catalyst. The conversion of nRP into RP was discovered to occur through the process of oxidation of nRP, facilitated by photocatalysis. While the quantification of RP and nRP was not performed in the present study, the increase in phosphorus removal from 10% to 60% when using the  $H_2O_2$ /US/HPC hybrid supports the hypothesis that the majority of nRP present in PSW was oxidized into RP under the combined influence of UV irradiation and US, with minimal phosphorus adsorption occurring on the nanocatalyst.

As depicted in Figure 3(b) and Figure 4(d), the rise of catalyst concentration from 0.5 to 1.5 g/L resulted in a notable escalation in phosphorus removal efficiency. The observed phenomenon can be attributed to the rise in photocatalyst nanoparticle concentration, leading to an enhancement in photon absorption and pollutant molecule adsorption. Additionally, the increased surface area of nanoparticles facilitates the generation of radicals by providing more active sites (Ertugay and Acar, 2015). Despite the fact that only 17% of  $PO_4$ -P was removed with US processing, 60% of  $PO_4$ -P was removed during the study. The use of photocatalyst particles in the US treatment has been well acknowledged to enhance the cavitation phenomena. This is attributed to the tendency of micro bubbles to fragment into smaller ones, thus leading to an enhanced total amount of regions characterized by high temperature and pressure (Cheng *et al.*, 2012). Additionally, there exists empirical evidence indicating that ultrasound shock waves have the potential to induce catalyst deposition and cleaning processes (Disselkamp *et al.*, 2004). Moradi *et al.* (2023) have observed that the occurrence of cavitation bubble collapse in the vicinity of nanoparticles during the process of photocatalysis leads to the production of asymmetric shock waves. Consequently, this process leads to the disintegration of particles and enables

the ongoing purification of the surface. As a result, there is a noticeable increase in the exposure of active sites on the surface of the material. According to the data presented in Figure 3(b) and Figure 4(b), there is a decline in phosphorus removal efficiency as the concentration of the catalyst is increased from 1.5 to 2.5 g/L. Consistent with prior research conducted by Dogdu (2022), our findings indicate that the effectiveness of degradation is significantly influenced by the extent of the available catalytic surface area and is constrained by the turbidity of the suspension, as noted by Paustian *et al.* (2022). Dogdu (2022) and Khan *et al.* (2023) both stated that an increase in the concentration of the catalyst results in a decrease in the propagation of ultrasonic waves inside the solution. Additionally, this increase in concentration promotes catalyst aggregation, which hinders the penetration of light due to light scattering, resulting in the loss of active sites. This loss is attributed to the formation of  $OH^\cdot$  in the solution, which acts as a shield and inhibits the accessibility of the active sites. Although there was no statistically significant difference between  $TiO_2$  and ZnO photocatalyst species in terms of phosphorus removal, this may be due to the greater specific surface area of  $TiO_2$  in comparison to ZnO.

Moreover, the data presented in Figure 3(b) indicates a positive correlation between the duration of the  $H_2O_2$ /US/HPC process and the effectiveness of phosphorus removal. Specifically, there was an increase in phosphorus removal efficiency from 30 to 105 min. The observed enhancement in the photocatalytic degradation of phosphorus, as a function of both sonication and illumination time, can be attributed to several factors. Firstly, sonication facilitates the thorough mixing of the substrate with the photocatalysts, ensuring a more uniform distribution of phosphorus throughout the reaction mixture. This increased contact between phosphorus and the catalysts promotes a more efficient degradation. Additionally, the prolonged illumination time allows for a greater number of photon-catalyst interactions, leading to an overall increase in degradation efficiency. However, phosphorus removal efficiency decreased significantly after 105 min. This is because the photoactivity of the photocatalyst is generally determined by the electron/hole pair generation, recombination, interfacial transfer processes, and surface reactions of these charge carriers with species adsorbed on the photocatalyst surface (Minero *et al.*, 2013). One additional factor contributing to the decline in phosphorus removal effectiveness after



105 min is the inability of nanocatalysts to adsorb RP and oxidized NRP, which are produced as a result of UV irradiation and US activities. Echavia *et al.* (2009) declared that the adsorption process, followed by a 60 min exposure to UV radiation, resulted in the total elimination of 0.1 mM glyphosate. No RP release was observed after the oxidation of glyphosate, indicating that orthophosphate and other intermediate chemicals that were liberated were effectively eliminated through adsorption.

### Cost analysis

The assessment of the economic implications of the technology employed in industrial companies plays a crucial role in assessing the feasibility and practicality of implementing such technology in real-world settings. There is little knowledge on the economic aspect of real wastewater treatment by H<sub>2</sub>O<sub>2</sub>/US/HPC. The addition of an ultrasonic device that consumes additional electricity in relation to the conventional PC system may raise performance and cost-effectiveness concerns (Rodrigues *et al.*, 2013). pH, catalyst concentration, and operation time are critical factors that significantly influence the efficiency of nutrient removal in the H<sub>2</sub>O<sub>2</sub>/US/HPC process, directly impacting the specific removal costs associated with it. In this study, only the expenses associated with the chemicals, specifically the costs of reagents and energy were taken into account for the purpose of calculating the overall cost of the process. The operating cost was calculated by adding up the costs of hydrogen peroxide, TiO<sub>2</sub> or ZnO

catalysts, and energy consumption, as shown in the following equation:

$$\text{Operating cost} = \text{cost}_{\text{H}_2\text{O}_2} + \text{cost}_{\text{TiO}_2/\text{ZnO}} + \text{cost}_{\text{energy}} \quad (1)$$

The cost of total consumed hydrogen peroxide, total consumed power (kWh), and total electricity consumption were calculated for each kg of NH<sub>4</sub><sup>+</sup>-N and PO<sub>4</sub>-P removal, which represents the maximum mineralization of PSW (\$/g), according to following equations (Rodrigues *et al.*, 2013; Asha *et al.*, 2015):

$$\text{cost}_{\text{H}_2\text{O}_2} = \frac{\text{price}_{\text{H}_2\text{O}_2} \left( \frac{\$}{\text{mL}} \right) [\text{H}_2\text{O}_2] \times 10^{-6} \left( \frac{\text{mL}}{\mu\text{L}} \right) \times \rho_{\text{H}_2\text{O}_2} \left( \frac{\text{kg}}{\text{L}} \right)}{\frac{\% \text{H}_2\text{O}_2}{100} \left( \frac{\text{kg}}{\text{L}} \right)} \quad (2)$$

$$\text{Total consumed power} = \frac{\text{consumed power (W)} \times \text{reaction time (min)}}{(100 \times 60)} \quad (3)$$

$$\text{cost}_{\text{energy}} (\$/\text{g}) = \frac{\text{total consumed power (kWh)} \times \text{unit cost of power} \left( \frac{\$}{\text{kWh}} \right)}{(\text{C}_{\text{influent,pollutant}} - \text{C}_{\text{effluent,pollutant}}) \left( \frac{\text{mg}}{\text{L}} \right) \times \text{operating volume (L)}} \times 10^3 \left( \frac{\text{mg}}{\text{g}} \right) \quad (4)$$

Chemicals (i.e., reagents and catalysts) obtained from Sigma-Aldrich®, electricity costs, and the electrical power of the devices used were as follows: H<sub>2</sub>O<sub>2</sub> (30% w/v, density at 30 °C = 1.11 kg/L), 76.43 US\$/100 mL; 0.17US\$/1 g of ZnO; the price of electricity is determined as 0.10US\$/kWh for industries by the Turkish Energy Market Regulatory Authority in October 2023; 0.06 kW for 2 peristaltic pumps, 0.003 kW air pump, 0.120 kW ultrasonic bath, and 0.036 kW UV lamp. Table 6 presents a comprehensive analysis of chemical and electrical energy utilization derived from experimental data, in which the H<sub>2</sub>O<sub>2</sub>/US/HPC process was employed to accomplish optimal removal of ammonia and phosphorus.

**Table 6** – Total chemical and electricity consumption costs for 1 g of NH<sub>4</sub><sup>+</sup>-N and PO<sub>4</sub>-P removal for the SPC process.

Exp No	ZnO (g)	H <sub>2</sub> O <sub>2</sub> (μL)	ZnO (US\$)	H <sub>2</sub> O <sub>2</sub> (US\$)	Chemical cost (US\$)	Cost of electrical consumption (US\$/g NH <sub>4</sub> <sup>+</sup> -N)	Cost of electrical consumption (US\$/g PO <sub>4</sub> -P)
1	2.5	0.002	0.42	0.00043	0.42	2.67	-
2	1.5	0.001	0.26	0.00011	0.26	-	2.14

The chemical costs are equal to the sum of the catalyst and H<sub>2</sub>O<sub>2</sub> used in the experiments. Moreover, the total electrical power consumed is equal to the sum of the electrical powers of the ultrasonic bath, UV lamp, air pump, and peristaltic pumps. According to Table 6, in Experiment 1, where optimum ammonium-N was removed from raw PSW by an ultrasound-assisted heterogeneous photocatalysis process, approximately 90% of the total cost was due to electrical energy consumption compared to chemical consumption. Since it was determined that the catalyst type was not statistically significant for optimal phosphorus removal, the less expensive ZnO was chosen instead of TiO<sub>2</sub>. Similarly, according to the results of experiment

2, in which optimal phosphorus removal (60%) was attained, 92% of the total cost was attributed to electricity consumption, while the remainder was attributed to nanocatalyst costs.

## CONCLUSIONS

In the present study, an environmentally friendly, low-cost, combined H<sub>2</sub>O<sub>2</sub>/US/HPC system was designed and implemented for the removal of ammonia and phosphorus from PSW. The key outcomes were as follows:

1. pH, catalyst concentration, and operating time were the primary operational variables



that significantly influenced the removal of ammonium-N and phosphorus in an integrated  $H_2O_2$ /US/HPC system. Even though the same type of effluent and reactor system was utilized, the optimal operating parameters varied based on the pollutant parameters. The optimal pH for ammonium-N removal was 10, while the optimal pH for phosphorus removal was 2.

- Multiple chemical and physical events, such as radical-producing reactions, hydroxylation, cavitation, ultrasound, increased mass transport, surface cleaning, and physical surface adsorption capacity, are likely to occur simultaneously and play a significant role in the enhancement of ammonia and phosphorus removal efficiency. Therefore, by combining  $H_2O_2$  and US with the HPC method, it was possible to eliminate the primary limitations encountered in the photocatalysis process for the removal of pollutants, such as catalyst fouling or mass transfer resistance, without affecting the morphology, structure, or crystallinity of the nanocatalyst.
- Ammonia and phosphorus removal efficiencies of processes such as single catalysis, sonolysis, and photolysis were between 9 and 19% on average, while the  $H_2O_2$ /US/HPC process increased this to an average of 50–60%. Nevertheless, despite the sufficient 180-min duration for achieving maximum degradation of  $NH_4^+$ -N, and  $PO_4$ -P, the average removal efficiency of these parameters (50% to 60%) might be attributed to interactions between different kinds of pollutants in real wastewater system, which might complicate the sonophotocatalytic degradation process. Pollutant removal efficiencies could also be affected by the accumulation of high concentrations of intermediate products after degradation of recalcitrant compounds in PSW.
- Scaled-up processes demand a more thorough economic analysis before employing this technique. The estimated cost analysis came from bench scale experiments which weren't good indicators of real-world cost-effectiveness.  $H_2O_2$ /US/HPC effluent degradation is heavily dependent on electrical energy consumption. Other costs (such as the cost of reactors, chemicals, etc.) must be considered and minimized without sacrificing performance.
- The  $H_2O_2$ /US/HPC hybrid method proposed in this study achieved an average ammonia and phosphorus removal rate of 50–60%, and

although this removal efficiency was below the permissible values, this integrated advanced treatment technique is proposed as a pre-treatment and/or post-treatment step for the treatment of PSWs with high organic pollutants and nutrient content.

- The results are consistent with previous literature and may open up a new and feasible direction towards an environmentally friendly treatment of poultry processing wastewater for poultry researchers and the poultry industry.

## FUNDING

This work was partially supported financially by Bolu Abant İzzet Baysal University Scientific Research, under grant number 2021.09.02.1498.

## DATA AVAILABILITY STATEMENT

No additional data are available.

## ACKNOWLEDGMENTS

The author extends their appreciation to Nazmiye Ebru Şen for her invaluable help in sampling wastewater and for her efforts during the laboratory work.

## CONFLICTS OF INTEREST

The author declares that there are no conflicts of interest regarding the publication of this article.

## REFERENCES

- Abdelhay A, Othman AA, Albsoul A. Treatment of slaughterhouse wastewater using high-frequency ultrasound: optimization of operating conditions by RSM. *Environmental Technology* 2020;42:4170–8. <https://doi.org/10.1080/09593330.2020.1746409>.
- Adewuyi YG. Sonochemistry in environmental remediation. 1. Combinative and hybrid sonophotochemical oxidation processes for the treatment of pollutants in water. *Environmental Science & Technology* 2005;39:3409–20. <https://doi.org/10.1021/es049138y>.
- Al-Bsoul A, Al-Shannag M, Tawalbeh M, *et al* Optimal conditions for olive mill wastewater treatment using ultrasound and advanced oxidation processes. *Science of The Total Environment* 2020;700:134576. <https://doi.org/10.1016/j.scitotenv.2019.134576>.
- APHA, AWWA, WEF. Standard methods for the examination of water and wastewater. 23<sup>rd</sup> ed. New York; 2017.
- Asha RC, Vishnuganth MA, Remya N, *et al* Livestock wastewater treatment in batch and continuous photocatalytic systems: performance and economic analyses. *Water, Air, & Soil Pollution* 2015;226. <https://doi.org/10.1007/s11270-015-2396-4>.
- Avula RY, Nelson HM, Singh RK. Recycling of poultry process wastewater by ultrafiltration. *Innovative Food Science & Emerging Technologies* 2009;10:1–8. <https://doi.org/10.1016/j.ifset.2008.08.005>.



- Balachandran R, Patterson Z, Deymier P, *et al* Understanding acoustic cavitation for sonolytic degradation of p-cresol as a model contaminant. *Chemosphere* 2016;147:52–9. <https://doi.org/10.1016/j.chemosphere.2015.12.066>.
- Bayar S, Yildiz YŞ, Yılmaz AE, *et al* The effect of stirring speed and current density on removal efficiency of poultry slaughterhouse wastewater by electrocoagulation method. *Desalination* 2011;280:103–7. <https://doi.org/10.1016/j.desal.2011.06.061>.
- Bazrafshan E, Kord Mostafapour F, *et al* Slaughterhouse wastewater treatment by combined chemical coagulation and electrocoagulation process. *PLoS ONE* 2012;7(6):e40108. <https://doi.org/10.1371/journal.pone.0040108>.
- Besharati Fard M, Mirbagheri SA, Pendashteh A. Removal of TCOD and phosphate from slaughterhouse wastewater using Fenton as a post-treatment of a UASB reactor. *Journal of Environmental Health Science and Engineering* 2020;18:413–22. <https://doi.org/10.1007/s40201-020-00469-w>.
- Bustillo-Lecompte CF, Ghafoori S, Mehrvar M. Photochemical degradation of an actual slaughterhouse wastewater by continuous UV/H<sub>2</sub>O<sub>2</sub> photoreactor with recycle. *Journal of Environmental Chemical Engineering* 2016;4:719–32. <https://doi.org/10.1016/j.jece.2015.12.009>.
- Bustillo-Lecompte CF, Mehrvar M. Slaughterhouse wastewater characteristics, treatment, and management in the meat processing industry: a review on trends and advances. *Journal of Environmental Management* 2015;161:287–302. <https://doi.org/10.1016/j.jenvman.2015.07.008>.
- Cao ST, Tran HP, Le HTT, *et al*. Impacts of effluent from different livestock farm types (pig, cow, and poultry) on surrounding water quality: a comprehensive assessment using individual parameter evaluation method and water quality indices. *Environmental Science and Pollution Research* 2021;28:50302–15. <https://doi.org/10.1007/s11356-021-14284-9>.
- Chakhtouna H, Benzeid H, Zari N, *et al*. Recent progress on Ag/TiO<sub>2</sub> photocatalysts: photocatalytic and bactericidal behaviors. *Environmental Science and Pollution Research* 2021;28:44638–66. <https://doi.org/10.1007/s11356-021-14996-y>.
- Cheng Z, Quan X, Xiong Y, *et al*. Synergistic degradation of methyl orange in an ultrasound intensified photocatalytic reactor. *Ultrasonics Sonochemistry* 2012;19:1027–32. <https://doi.org/10.1016/j.ultrsonch.2012.02.008>.
- Cho SP, Hong SC, Hong S-I. Photocatalytic degradation of the landfill leachate containing refractory matters and nitrogen compounds. *Applied Catalysis B: Environmental* 2002;39:125–33. [https://doi.org/10.1016/s0926-3373\(02\)00079-6](https://doi.org/10.1016/s0926-3373(02)00079-6).
- Choi SJ, Kim B-K, Lee T-H, *et al*. Electrical and thermoelectric transport by variable range hopping in thin black phosphorus devices. *Nano Letters* 2016;16:3969–75. <https://doi.org/10.1021/acs.nanolett.5b04957>.
- Conte F, Pellegatta V, Tripodi A, *et al*. Photo-oxidation of ammonia to molecular nitrogen in water under UV, Vis and sunlight irradiation. *Catalysts* 2021;11:975. <https://doi.org/10.3390/catal11080975>.
- Dadi D, Mengistie E, Terefe G, *et al*. Assessment of the effluent quality of wet coffee processing wastewater and its influence on downstream water quality. *Ecology & Hydrobiology* 2018;18:201–11. <https://doi.org/10.1016/j.ecohyd.2017.10.007>.
- Davarnejad R, Nasiri S. Slaughterhouse wastewater treatment using an advanced oxidation process: optimization study. *Environmental Pollution* 2017;223:1–10. <https://doi.org/10.1016/j.envpol.2016.11.008>.
- Dikmen E, Dogdu G, Yalcuk A. Comparison performances of hybrid sonocatalysis and sonophotocatalysis on the elimination of 2,4-Dichlorophenoxyacetic acid in water: mineralization and economic analysis. *Polish Journal of Environmental Studies* 2022;31:4589–602. <https://doi.org/10.15244/pjoes/149575>.
- Disselkamp RS, Judd KM, Hart TR, *et al*. A comparison between conventional and ultrasound-mediated heterogeneous catalysis: hydrogenation of 3-buten-1-ol aqueous solutions. *Journal of Catalysis* 2004;221:347–53. <https://doi.org/10.1016/j.jcat.2003.08.008>.
- Dogdu G, Sen NE. An innovative solution for the treatment of poultry industry wastewater with advanced hybrid technology sono-photocatalysis. *Global Nest Journal* 2022;25(2):95–105. <https://doi.org/10.30955/gnj.004305>.
- Dogdu G. An eco-friendly hybrid sonophotocatalytic approach to optimize carpet washing wastewater treatment. *Desalination and Water Treatment* 2022;262:60–73. <https://doi.org/10.5004/dwt.2022.28454>.
- DogduOkcu G, Tunacan T, Dikmen E. Photocatalytic degradation of yellow 2G dye using titanium dioxide/ultraviolet A light through a Box–Behnken experimental design: Optimization and kinetic study. *Journal of Environmental Science and Health, Part A* 2019;54:136–45. <https://doi.org/10.1080/10934529.2018.1530540>.
- Echavia GRM, Matzusawa F, Negishi N. Photocatalytic degradation of organophosphate and phosphonoglycine pesticides using TiO<sub>2</sub> immobilized on silica gel. *Chemosphere* 2009;76:595–600. <https://doi.org/10.1016/j.chemosphere.2009.04.055>.
- Ertugay N, Acar FN. Decolorization of direct blue 71 using UV irradiation and ultrasound in the presence of TiO<sub>2</sub> catalyst. *Desalination and Water Treatment* 2015;57:9318–24. <https://doi.org/10.1080/19443994.2015.1041050>.
- FAO. Meat and meat products [cited 2023 Aug 29]. Available from: [https://www.fao.org/3/cb9427en/cb9427en\\_meat.pdf](https://www.fao.org/3/cb9427en/cb9427en_meat.pdf) Available: 29 August 2023.
- Fatima F, Du H, Kommalapati RR. Treatment of poultry slaughterhouse wastewater with membrane technologies: a review. *Water* 2021;13:1905. <https://doi.org/10.3390/w13141905>.
- García-Prieto JC, González-Burciaga LA, Proal-Nájera JB, *et al*. Kinetic study and modeling of the degradation of aqueous ammonium/ammonia solutions by heterogeneous photocatalysis with TiO<sub>2</sub> in a UV-C pilot photoreactor. *Catalysts* 2022;12:352. <https://doi.org/10.3390/catal12030352>.
- Gay SW, Knowlton KF. Ammonia emissions and animal agriculture [publication 442-110]. Virginia: Virginia State University, Blacksburg; 2005.
- Gong X, Wang H, Yang C, *et al*. Photocatalytic degradation of high ammonia concentration wastewater by TiO<sub>2</sub>. *Future Cities Environment* 2015;1:12.
- Gray CW, McDowell RW, Condon LM, *et al*. Changes in soil cadmium concentrations with time following cessation of phosphorus fertilizer inputs. *Journal of Environmental Quality* 2020;49:1054–61. <https://doi.org/10.1002/jeq2.20086>.
- Hajaya MG, Pavlostathis SG. Modeling the fate and effect of benzalkonium chlorides in a continuous-flow biological nitrogen removal system treating poultry processing wastewater. *Bioresource Technology* 2013;130:278–87. <https://doi.org/10.1016/j.biortech.2012.11.103>.
- Hernández S, Hidalgo D, Sacco A, *et al*. Comparison of photocatalytic and transport properties of TiO<sub>2</sub> and ZnO nanostructures for solar-driven water splitting. *Physical Chemistry Chemical Physics* 2015;17:7775–86. <https://doi.org/10.1039/c4cp05857g>.



- Jagannathan M, Jayaraman T, Dhandapani B, *et al.* Hybrid advanced oxidation processes involving ultrasound: an overview. *Molecules* 2019;24:3341. <https://doi.org/10.3390/molecules24183341>.
- Jandaghian F, Ebrahimi Pirbazari A, Tavakoli O, *et al.* Comparison of the performance of Ag-deposited ZnO and TiO<sub>2</sub> nanoparticles in levofloxacin degradation under UV/visible radiation. *Journal of Hazardous Materials Advances* 2023;9:100240. <https://doi.org/10.1016/j.hazadv.2023.100240>
- Kang J, Amoozegar A, Hesterberg D, *et al.* Phosphorus leaching in a sandy soil as affected by organic and inorganic fertilizer sources. *Geoderma* 2011;161:194–201. <https://doi.org/10.1016/j.geoderma.2010.12.019>.
- Khan K, Khitab F, Shah J, *et al.* Ultrasound assisted photocatalytic degradation of isoproturon and triasulfuron herbicides using visible light driven impregnated zinc oxide catalysts. *Sustainable Environment Research* 2023;33. <https://doi.org/10.1186/s42834-023-00184-9>.
- LI W, WU D, SHI X, *et al.* Removal of organic matter and ammonia nitrogen in azodicarbonamide wastewater by a combination of power ultrasound radiation and hydrogen peroxide. *Chinese Journal of Chemical Engineering* 2012;20:754–9. [https://doi.org/10.1016/s1004-9541\(11\)60245-0](https://doi.org/10.1016/s1004-9541(11)60245-0).
- Mapukata S, Ntsendwana B, Mokhena T, *et al.* Advances on sonophotocatalysis as a water and wastewater treatment technique: efficiency, challenges and process optimisation. *Frontiers in Chemistry*, 2023;11. <https://doi.org/10.3389/fchem.2023.1252191>.
- Mayer BK, Baker LA, Boyer TH, *et al.* Total value of phosphorus recovery. *Environmental Science and Technology* 2016;50(13):6606–6620. <https://doi.org/10.1021/acs.est.6b01239>.
- Meiramkulova K, Jakupova Z, Orynbekov D, *et al.* Evaluation of electrochemical methods for poultry slaughterhouse wastewater treatment. *Sustainability* 2020;12:5110. <https://doi.org/10.3390/su12125110>.
- Minero C, Maurino V, Vione D. Photocatalytic mechanisms and reaction pathways drawn from kinetic and probe molecules. *Photocatalysis and Water Purification* 2013;53–72. <https://doi.org/10.1002/9783527645404.ch3>.
- Moharami S, Jalali M. Effect of TiO<sub>2</sub>, Al<sub>2</sub>O<sub>3</sub>, and Fe<sub>3</sub>O<sub>4</sub> nanoparticles on phosphorus removal from aqueous solution. *Environmental Progress & Sustainable Energy* 2014;33:1209–19. <https://doi.org/10.1002/ep.11917>.
- Moradi S, Rodriguez-Secco C, Hayati F, *et al.* Sonophotocatalysis with photoactive nanomaterials for wastewater treatment and bacteria disinfection. *ACS Nanoscience Au* 2023;3:103–29. <https://doi.org/10.1021/acsnanoscienceau.2c00058>.
- Mousazadeh M, Niaragh EK, Usman M, *et al.* A critical review of state-of-the-art electrocoagulation technique applied to COD-rich industrial wastewaters. *Environmental Science and Pollution Research* 2021;28:43143–72. <https://doi.org/10.1007/s11356-021-14631-w>.
- Musa MA, Idrus S. Physical and biological treatment technologies of slaughterhouse wastewater: a review. *Sustainability* 2021;13:4656. <https://doi.org/10.3390/su13094656>.
- Ngobeni PV, Gutu L, Basitere M, *et al.* Poultry slaughterhouse wastewater treatment using an integrated biological and electrocoagulation treatment system: process optimisation using response surface methodology. *Sustainability* 2022;14:9561. <https://doi.org/10.3390/su14159561>.
- OECD. Meat consumption (indicator) [cited 2023 Aug 29]. Available from: <https://doi.org/10.1787/fa290fd0-en>.
- Ozturk E, Bal N. Evaluation of ammonia–nitrogen removal efficiency from aqueous solutions by ultrasonic irradiation in short sonication periods. *Ultrasonics Sonochemistry* 2015;26:422–7. <https://doi.org/10.1016/j.ultsonch.2015.02.012>.
- Panda D, Manickam S. Recent advancements in the sonophotocatalysis (SPC) and doped-sonophotocatalysis (DSPC) for the treatment of recalcitrant hazardous organic water pollutants. *Ultrasonics Sonochemistry* 2017;36:481–96. <https://doi.org/10.1016/j.ultsonch.2016.12.022>.
- Patidar R, Srivastava VC. Ultrasound-induced intensification of electrochemical treatment of bulk drug pharmaceutical wastewater. *ACS ES&T Water* 2021;1:1941–54. <https://doi.org/10.1021/acsestwater.1c00159>.
- Paustian D, Franke M, Stelter M, *et al.* Sonophotocatalysis - limits and possibilities for synergistic effects. *Catalysts* 2022;12:754. <https://doi.org/10.3390/catal12070754>.
- Purwono P, Hadiyanto H, Budihardjo MA. Equilibrium of ammonia (NH<sub>3</sub>) and ammonium (NH<sub>4</sub><sup>+</sup>) during microalgae harvesting using electrocoagulation. *International Journal of Engineering* 2023;36:565–72. <https://doi.org/10.5829/ije.2023.36.03c.17>.
- Rinquest Z, Basitere M, Ntwampe SKO, *et al.* Poultry slaughterhouse wastewater treatment using a static granular bed reactor coupled with single stage nitrification-denitrification and ultrafiltration systems. *Journal of Water Process Engineering* 2019;29:100778. <https://doi.org/10.1016/j.jwpe.2019.02.018>.
- Rodrigues GC, Paredes P, Gonçalves JM, *et al.* Comparing sprinkler and drip irrigation systems for full and deficit irrigated maize using multicriteria analysis and simulation modelling: Ranking for water saving vs. farm economic returns. *Agricultural Water Management* 2013;126:85–96. <https://doi.org/10.1016/j.agwat.2013.05.005>.
- Shahedi A, Darban AK, Taghipour F, *et al.* A review on industrial wastewater treatment via electrocoagulation processes. *Current Opinion in Electrochemistry* 2020;22:154–69. <https://doi.org/10.1016/j.coelec.2020.05.009>.
- Silva AMT, Nouli E, Carmo-Apolinário ÂC, *et al.* Sonophotocatalytic/H<sub>2</sub>O<sub>2</sub> degradation of phenolic compounds in agro-industrial effluents. *Catalysis Today* 2007;124:232–9. <https://doi.org/10.1016/j.cattod.2007.03.057>.
- Sivasankar T, Moholkar VS. Physical insights into the sonochemical degradation of recalcitrant organic pollutants with cavitation bubble dynamics. *Ultrasonics Sonochemistry* 2009;16:769–81. <https://doi.org/10.1016/j.ultsonch.2009.02.009>.
- Sousa MRS, Lora-García J, López-Pérez M-F, *et al.* Operating conditions optimization via the taguchi method to remove colloidal substances from recycled paper and cardboard production wastewater. *Membranes* 2020;10:170. <https://doi.org/10.3390/membranes10080170>.
- Suslick KS. The chemical effects of ultrasound. *Scientific American* 1989;260:80–6. <https://doi.org/10.1038/scientificamerican0289-80>.
- Terán Hilarés R, Atoche-Garay DF, Pinto Pagaza DA, *et al.* Promising physicochemical technologies for poultry slaughterhouse wastewater treatment: a critical review. *Journal of Environmental Chemical Engineering* 2021;9:105174. <https://doi.org/10.1016/j.jece.2021.105174>.
- Toh YP, Bashir MJK, Guo X, *et al.* Advanced treatment of poultry slaughterhouse wastewater using electrocoagulation and peroxidation: parametric analysis and process optimization. *International Journal of Environmental Science and Technology* 2023;20:12307–22. <https://doi.org/10.1007/s13762-023-04824-w>.



- Topcu NS, Duman G, Olgun H, *et al.* Evaluation of poultry manure: combination of phosphorus recovery and activated carbon production. *ACS Omega* 2022;7:20710–8. <https://doi.org/10.1021/acsomega.2c00975>.
- Türkdoğan FI, Yetilmezsoy K, Goncaloğlu BI, *et al.* Removal of ammonium nitrogen from the daf-pretreated poultry slaughterhouse wastewater by *lemna minor*. *Proceedings of the 4th International Conference on Engineering and Natural Science*; Kyiv, Ukraine; 2018. p.1-8.
- Turkten N, Bekbolet M. Photocatalytic performance of titanium dioxide and zinc oxide binary system on degradation of humic matter. *Journal of Photochemistry and Photobiology A: Chemistry* 2020;401:112748. <https://doi.org/10.1016/j.jphotochem.2020.112748>.
- Wang G, Cheng H. Application of photocatalysis and sonocatalysis for treatment of organic dye wastewater and the synergistic effect of ultrasound and light. *Molecules* 2023;28:3706. <https://doi.org/10.3390/molecules28093706>.
- Wang S, Wu X, Wang Y, *et al.* Removal of organic matter and ammonia nitrogen from landfill leachate by ultrasound. *Ultrasonics Sonochemistry* 2008;15:933–7. <https://doi.org/10.1016/j.ultsonch.2008.04.006>.
- Williams Y, Basitere M, Ntwampe SKO, *et al.* Application of response surface methodology to optimize the COD removal efficiency of an EGSB reactor treating poultry slaughterhouse wastewater. *Water Practice and Technology* 2019;14:507–14. <https://doi.org/10.2166/wpt.2019.032>.
- Woodard, F. *Industrial waste treatment handbook*. Boston, MA: Butterworth Heinemann; 2001. Available from: [http://books.google.ie/books?id=G4tTOESKvpuC&printsec=frontcover&dq=Industrial+Waste+Treatment+Handbook&hl=&cd=1&source=gbs\\_api](http://books.google.ie/books?id=G4tTOESKvpuC&printsec=frontcover&dq=Industrial+Waste+Treatment+Handbook&hl=&cd=1&source=gbs_api)
- Wu C-Q, Zhang Y, Chen X. Ammonia removal mechanism by the combination of air stripping and ultrasound as the function of pH. *Earth and Environmental Science* 2019;344:012051. <https://doi.org/10.1088/1755-1315/344/1/012051>.
- Xu J, Jia J, Wang J. Ultrasonic decomposition of ammonia-nitrogen and organic compounds in coke plant wastewater. *Journal of the Chinese Chemical Society* 2005;52:59–65. <https://doi.org/10.1002/jccs.200500009>.
- Yaakob MA, Mohamed RMSR, Al-Gheethi AAS, *et al.* Characteristics of chicken slaughterhouse wastewater. *Chemical Engineering Transaction* 2018;63:637-42. <https://doi.org/10.3303/CET1863107>.
- Yang X, Wang Y, Li CM, *et al.* Mechanisms of water oxidation on heterogeneous catalyst surfaces. *Nano Research* 2021;14:3446–57. <https://doi.org/10.1007/s12274-021-3607-5>.
- Yeoh JX, Md. Jamil SNA, Syukri F, *et al.* Comparison between conventional treatment processes and advanced oxidation processes in treating slaughterhouse wastewater: a review. *Water* 2022;14:3778. <https://doi.org/10.3390/w14223778>.
- Yu R, Yu X, Fu J, *et al.* Removal of ammonia nitrogen in aquaculture wastewater by composite photocatalyst TiO<sub>2</sub>/carbon fibre. *Water and Environment Journal* 2021;35:962–70. <https://doi.org/10.1111/wej.12686>.